



## Anion-exchange membranes in lithium extraction by means of capacitive deionization system

Anna Siekierka<sup>a,\*</sup>, Joanna Wolska<sup>a</sup>, Marek Bryjak<sup>a</sup>, Wojciech Kujawski<sup>b</sup>

<sup>a</sup>Wrocław University of Technology, Faculty of Chemistry, 27 Wyb. Wyspińskiego, 50-370 Wrocław, Poland, emails: [anna.siekierka@pwr.edu.pl](mailto:anna.siekierka@pwr.edu.pl) (A. Siekierka), [joanna.wolska@pwr.edu.pl](mailto:joanna.wolska@pwr.edu.pl) (J. Wolska), [marek.bryjak@pwr.edu.pl](mailto:marek.bryjak@pwr.edu.pl) (M. Bryjak)

<sup>b</sup>Nicolaus Copernicus University in Torun, Faculty of Chemistry, 7 Gagarina Str., 87-100 Toruń, Poland, email: [kujawski@chem.umk.pl](mailto:kujawski@chem.umk.pl)

Received 30 June 2016; Accepted 5 December 2016

### ABSTRACT

In this paper, we evaluate extraction of lithium chloride by membrane capacitive deionization system composed of two electrodes: one prepared from lithium-selective adsorbent and one obtained from activated carbon and coated with anion-exchange membrane. Lithium-selective sorbent was prepared by solid-state reaction of lithium carbonate, manganese carbonates and titanium dioxide. The anion-exchange membranes were prepared by modifying poly(vinyl chloride) films with ethylenediamine. The chemical structure of membranes was investigated by Fourier transform infrared spectroscopy. The following membrane properties were determined: water regain, ion-exchange capacity, chloride and nitrogen contents. Taking into account the criteria of lithium sorption and desorption, the most efficient selective separation system was selected. It was found that salt adsorption capacity reached the average value of 34.2 mg/g<sub>electrode</sub> for LiCl, while for KCl and NaCl 8.6 mg/g<sub>electrode</sub> and 9.8 mg/g<sub>electrode</sub> respectively.

**Keywords:** Lithium adsorbent; Anion-exchange membrane; Selective capacitive deionization

### 1. Introduction

Lithium is a raw and critical element used in the production of: lithium ions batteries, glass, ceramics, metal alloys and applied for polymer syntheses. It can be acquired from two different sources: (i) extracted from minerals, salt lakes or underground brines and (ii) recovered from spent lithium ions batteries [1]. Almost 80% of the lithium comes from brines of the South America Salars where the weather conditions like solar radiation, low humidity and low rainfall allow to apply an evaporation method [2]. The process is based on pumping of brine into series of shallow ponds where a sequential precipitation of salts takes place. The whole process lasts 1–1.5 year [3]. Despite its simplicity, the technology suffers from the lack of production elasticity due to long time of lithium salt

manufacturing, large area of ponds, substantial water consumption, production of large quantities of wastes and strong impact on the environment. Hence, the search for other separation methods has become critical and many studies have been recently launched [4].

The following methods for lithium recovery have been evaluated: adsorption [5–11], liquid–liquid extraction [12–15], membrane electrolysis [16] and electro dialysis [17], ion-pumping [18], sorption–membrane hybrid process [19] and capacitive deionization (CDI) [20,21]. Among them the CDI [22,23], based on electrosorption of ions onto surface of porous electrode with formation of electrical double layer, has gained the growing attention. The studies on CDI efficiency have indicated the most important material properties: pore size distribution and charge of surface [24–27]. The effect of the charge has been investigated by coating of electrode with various oxides that

\* Corresponding author.

Presented at PERMEA 2016 (Membrane Science and Technology Conference of Visegrád Countries) and MELPRO 2016 (Membrane and Electromembrane Processes Conference), 15–19 May 2016, Prague, Czech Republic.

can develop charges in aqueous environment [28–31]. The use of chemically modified activated carbon for production of the electrodes could be considered as an alternative approach [32,33]. The second way to raise the CDI efficiency is to insert an ion-exchange membrane onto the front of the electrode [23,34]. That process is called membrane capacitive desalination (MCDI).

A few reports on the use of CDI/MCDI systems for separation on lithium from aqueous solutions have been published so far [20,21,35]. They were focused on the use of lithium selective electrode prepared from spinel of manganese oxide to collect lithium ions and carbon electrode for anions capturing. Anion-exchange membrane was added to that system to raise the separation efficiency. The evaluated systems showed good reproducibility and durability during the repeated adsorption/desorption cycles.

The goal of this paper is to show usefulness of the MCDI system for extraction of lithium chloride. In this evaluation, the system was composed of lithium capturing electrode, carbon electrode and anion-exchange membrane. The second goal of the paper was to show method for preparation of anion-exchange membrane that could improve lithium chloride extraction.

## 2. Materials and methods

### 2.1. Materials

Lithium adsorbent was prepared from  $\text{Li}_2\text{CO}_3$ ,  $\text{MnCO}_3$  and  $\text{TiO}_2$  purchased from Aldrich-Sigma (Poznan, Poland). The activated carbon, CWZ-22 delivered by Gryfskand (Gryfino, Poland), was used to prepare electrode for anions capturing. Membranes were prepared from poly(vinyl chloride) (PVC; Ongrovil® S-5167 with  $K$  value of 66–68) supplied by BorsodChem (Katowice, Poland). Ethylenediamine (EDA) was bought from Sigma. Cyclohexanone (CH), tetrahydrofuran (THF) and ethanol were delivered by Avantor Performance Materials (Gliwice, Poland).

### 2.2. Synthesis of lithium inorganic adsorbent

Lithium adsorbent was prepared at 500°C by a solid-state reaction of  $\text{Li}_2\text{CO}_3$ ,  $\text{MnCO}_3$  and  $\text{TiO}_2$  powders.  $\text{Li}_2\text{CO}_3$  to  $\text{MnCO}_3$  weight ratio was kept as 1–3 for all syntheses. Content of titanium dioxide was fixed at 10 wt%. Solid-state reaction took place in a vertical furnace heated at the rate of 40°C/min. The total time of reaction was fixed to 1 h. After the completion of the reaction, the precursor of lithium adsorbent was cooled to 25°C during 24 h and finally treated with large volume of 1 M aqueous HCl. The process was carried out for 24 h at room temperature. Finally, prepared sorbent was washed with distilled water, dried and ground to particles of 50  $\mu\text{m}$  size.

### 2.3. Preparation of electrode for capacitive deionization

All electrodes were prepared by mixing 90 wt% of lithium adsorbent or activated carbon with 10 wt% of PVC dissolved in CH (3.5 wt% solution of polymer). The obtained paste was stirred vigorously for 1 h at room temperature and degassed under vacuum (10 min, room temperature). Finally,

the slurry was cast on a graphite foil and formed in 120  $\mu\text{m}$  thick film. The evaporation of solvent was carried out overnight at normal pressure and completed in vacuum for 2 h. The electrodes were kept in deionization water (DI) water.

### 2.4. Preparation of PVC foils

Two types of PVC foil were prepared by means of wet method. PVC films were cast from 10 wt% tetrahydrofuran solution (10THF) or from 9 wt% cyclohexanone solution (9CH) onto a glass plate and dried at room temperature overnight. The thickness of obtained foils was  $50 \pm 3 \mu\text{m}$ .

### 2.5. Preparation of PVC membranes

Foils of PVC were kept in 10 mL of EDA for 7 d at room temperature. The conditions for membrane modification were selected previously [36]. After modification the obtained membranes were washed with ethanol, ethanol/water (1:1), water and alternately immersed in 1 M HCl and 1 M NaOH solutions.

### 2.6. CDI system

To study lithium sorption process, the Fumatech laboratory electro dialyzer FT-ED-100-4 was used. The stack consisted of two electrodes and one anion-exchange membrane. The scheme of the used CDI system is shown in Fig. 1.

To investigate the selectivity of the system, 10 mM aqueous solutions of LiCl, NaCl and KCl were used. The adsorption and desorption processes were carried out for 30 min at 25°C for all solutions. The cell was biased with voltage that changed from 0.5 to 3 V. The voltage was kept at the same value for adsorption and desorption with reversed polarity. All measurements were performed in triplicate.

Salt adsorption capacity (SAC) was defined as follows:

$$\text{SAC} = \frac{(C_o - C_f) \cdot V}{m} \quad (1)$$

where  $C_o$  (mg/dm<sup>3</sup>) and  $C_f$  (mg/dm<sup>3</sup>) are initial and final salt concentration,  $V$  (dm<sup>3</sup>) is the solution volume and  $m$  (g) is the mass of both electrodes.

### 2.7. Analytical section

#### 2.7.1. X-ray diffraction analysis

The structure of crystalline phases of inorganic lithium adsorbent was investigated by mean of X-ray diffraction (XRD). The measurements were performed in  $2\theta$  angle in the range of 5°–120°, at room temperature with 0.02° step and rate of 3°C/min. Philips X'Pert PW 3040/60 diffractometer ( $K\alpha = 1.5418 \text{ \AA}$ ) with Cu lamp (30 mA and 40 kV) was used. To acquire crystal grain size, the quantitative analysis of diffraction pattern with Scherrer equation was applied:

$$\tau = \frac{k \cdot \lambda}{B \cdot \cos\theta_B} \quad (2)$$

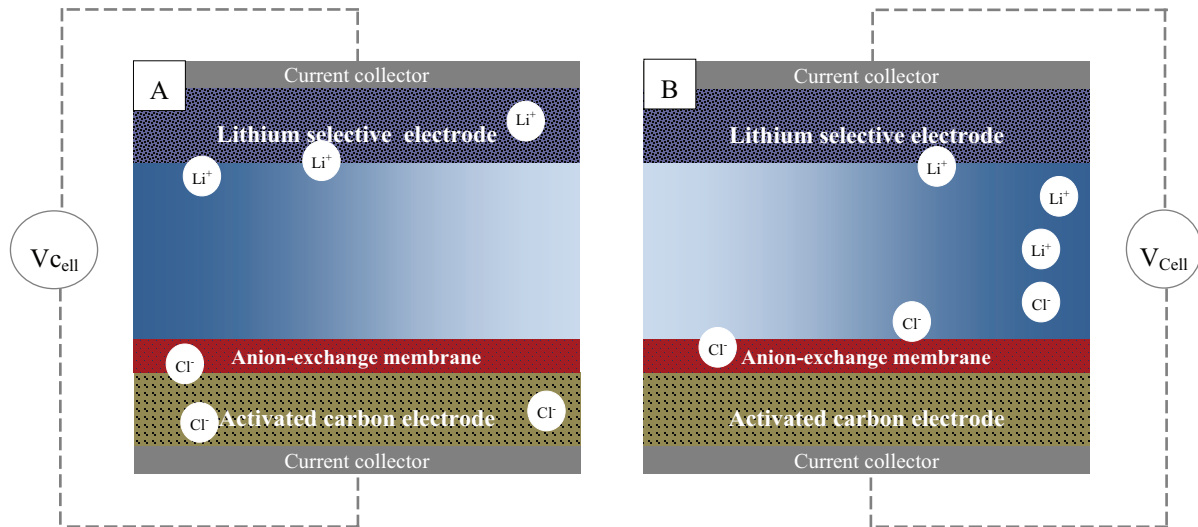


Fig. 1. Scheme of MCDI stack in (A) adsorption process and (B) desorption process.

where  $k$  is a dimensionless shape factor,  $\lambda$  is the X-ray wavelength,  $B$  is the line broadening at half the maximum intensity and  $\theta_B$  is the Bragg angle.

#### 2.7.2. Porosity of material

Porous texture of the materials was analyzed by  $N_2$  sorption at 77 K using Autosorb IQ gas sorption analyzer. The Brunauer–Emmett–Teller (BET) standard method was used to calculate the specific surface area from adsorption data when  $P/P_0$  changed from 0 to 1. Total pore volume of pores was estimated from the amount of nitrogen adsorbed at  $P/P_0 = 0.95$ .

#### 2.7.3. Fourier transform infrared spectroscopy

Prepared membranes were analyzed in the range of 4,000–300  $cm^{-1}$  by FTIR on the Vertex 70v vacuum spectrometer (Bruker Company, Coventry, England). In the analysis, 64 scans were collected. Polymer samples were prepared in KBr pellets.

### 2.8. Characterization of membranes

#### 2.8.1. Contact angle measurement

Static contact angles of water droplets were measured by goniometer PG-X (Fibro Systems Europe, Veenendaal, Netherlands). The measurements were repeated 20 times.

#### 2.8.2. Water regain

Water regain ( $W_{H_2O}$ ) of membranes was determined according to Eq. (3):

$$W_{H_2O} = \frac{(m_w - m_d)}{m_d} \quad (3)$$

where  $m_w$  is the weight of swollen membrane and  $m_d$  the weight of dry membrane.

#### 2.8.3. Ion-exchange capacity

Ion exchange capacity ( $Z_{IEC}$ ) was estimated on the basis of acid–base titration method and calculated according to Eq. (4):

$$Z_{IEC} = \frac{(C_b \times V_b - C_a \times V_a) \times A}{m_d} \quad (4)$$

where  $C_b$  and  $C_a$  are molar concentration of NaOH and HCl, respectively,  $V_b$  is the volume of NaOH taken to titration,  $V_a$  is the volume of HCl used for titration of NaOH solution,  $A$  is the volume correction (in our case 5) and  $m_d$  is the weight of dry membrane.

#### 2.8.4. Chloride content

Chloride content before and after modification was measured by burning about 20 mg of dry sample in a flask containing 3% hydrogen peroxide solution. The content of chloride was determined by the Schöniger's method [37].

#### 2.8.5. Nitrogen content

Nitrogen content in polymer was measured by the Kjeldahl's method after mineralization of the sample (about 200 mg) in concentrated sulfuric acid containing copper sulfate and potassium sulfate [38].

## 3. Results

### 3.1. XRD analysis

The structure of inorganic lithium adsorbent was determined by XRD.

Fig. 2(A) shows the XRD patterns for inorganic lithium adsorbent and Fig. 2(B) presents model of lithium manganese oxide hydroxide available under reference code 01-089-0755. The most prominent peak is at  $2\theta = 18.9^\circ$ , which corresponds to the reflection of (111) plane. The literature shows that diffusion of Li ion takes place mostly into some

octahedral sites and the (111) orientation allows lithium to better penetrate sorbent [36]. Obtained diffraction peaks at angle  $2\theta = 36^\circ$  and  $44^\circ$  are directly related to manganese oxides form while peaks at angle  $2\theta = 26^\circ$ ,  $82^\circ$  and  $84^\circ$  correspond to titanium oxide. All reflections attributed to the films correspond to Bragg positions for the spinel phase. Additionally, based on peaks with (111) reflection it was possible to calculate the mean size of crystalline domains. They were estimated at 3.88 Å. On the base of conducted studies, we assumed that by sintering of lithium and manganese carbonates with titanium dioxide, we obtained sorbent with homogenous morphology that was characterized by the structure similar to  $H_{0.6}Li_{0.08}Mn_{1.72}O_4$ .

### 3.2. Porosity and specific surface area of materials

The morphology and pore size of obtained materials were determined by means of BET isotherms of  $N_2$ . The data are shown in Table 1.

As it is seen, the lithium selective sorbent had poorly developed porous structure with low pore volume and small pores in comparison with activated carbon. The properties of CWZ-22 were typical for activated carbons used for the preparation of CDI electrodes [23].

### 3.3. IR spectroscopy

By applying EDA, it was possible to incorporate the ion-exchange groups into PVC films. However, the

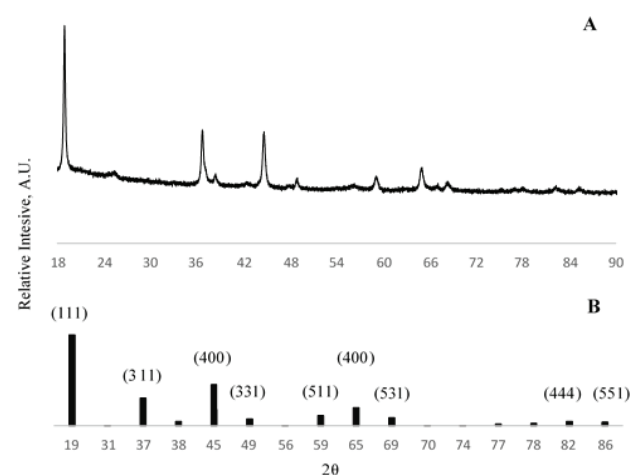


Fig. 2. XRD patterns for lithium inorganic adsorbent with 10 wt% content of titanium oxide.

Table 1

Surface areas, pore volume and pore sizes of materials used for electrode preparation

Samples	Specific surface area, $m^2/g$	Pore volume, $cm^3/g$	Pore diameter, nm
Lithium adsorbent	47	0.091	1.1
Activated carbon CWZ-22	977	0.491	<2

conditions of modifications should be very gentle; otherwise an undesirable crosslinking process might occur. To follow the effect of modification, the properties of unmodified and modified membranes were investigated by means of Fourier transform infrared (FTIR) spectroscopy that allowed to characterize the chemical composition of the obtained membranes. Fig. 3 shows the spectra. The absorption bands attributed to N–H (primary amines and secondary amines) groups were observed at wavelengths of  $3,346\text{ cm}^{-1}$  as a stretching vibrations and at  $1,610\text{ cm}^{-1}$  as bending vibrations. Strongly stretching vibration at  $2,900\text{ cm}^{-1}$ , corresponded to  $=C-H$  and  $=CH_2$ , could confirm the PVC dehydrochlorination with formation of unsaturated bounds [39].

The analysis of spectra allowed us to conclude that modification of PVC films with EDA took place either for films prepared from CH or films obtained from THF solutions and that obtained membranes had amine groups incorporated into the polymer structure.

### 3.4. Characterization of membranes

Modification with EDA caused the change of surface energy. To monitor these changes the surface wettability was evaluated by means of contact angle measurement. The values of contact angles are given in Table 2. It could be noted that modification improved water wettability manifested by a significant decrease of contact angle.

For extended characterization of obtained membranes, chloride and nitrogen contents, ion-exchange capacity and water regain were determined. It was observed that water regain increased for modified membranes and that aminated membranes had lower amounts of chloride atoms. What is more, both modified membranes had similar ion-exchange capacity.

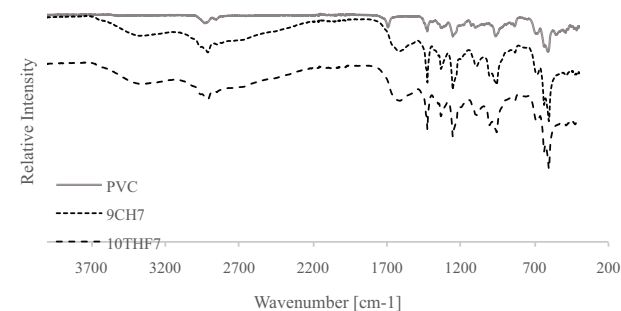


Fig. 3. IR spectra of PVC, 9CH7 and 10THF7 membranes.

Table 2

Properties of obtained membranes

Sample	$Z_{IEC}$ (mmol/g)	$Z_{Cl}$ (mmol/g)	$Z_N$ (mmol/g)	$W_{H_2O}$ (g/g)	$\theta_{H_2O}$ ( $^\circ$ )
9CH	0	15.5	0	0.5	75
9CH7	1.3	14.1	2.3	1.0	36
10THF	0	15.6	0	0.4	74
10THF7	1.4	14.2	2.4	1.1	35

3.5. Capacitive deionization

To evaluate the efficiency of lithium extraction in the presence of 10THF7 and 9CH7 membranes the MCDI process was carried out. The development of salt adsorption capacity with various voltage is shown in Fig. 4.

It can be seen that the highest value of electrosorption was observed for 2.5 V. It was about critical value of 1.2 V considered as the safe for CDI [23]. It seemed to us that the drop of voltage on ion-exchange membrane decreased the tendency of water to dissociate. What is more, carbon does not catalyze water dissociation and for some cases the high voltage does not generate hydrogen in the system [40]. This case was not verified in our study and for simplicity we took 2.5 V to run the sorption process in our MCDI stack.

Despite both membranes had similar ion-exchange capacity, the maximum value of salt adsorption was observed for 10THF7. It looked that both membranes could have different physical structure that could affect the transport of chloride ions. Such effect was better seen when sorption/desorption

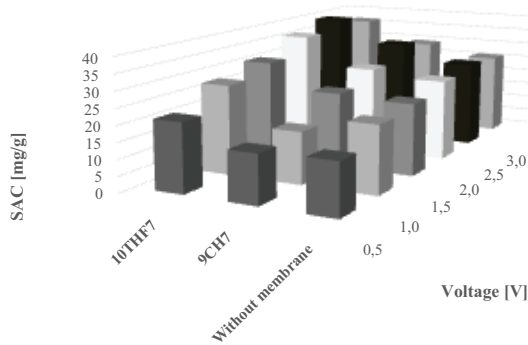


Fig. 4. Salt adsorption capacity of lithium chloride in CDI and MCDI stack with 10THF7 and 9CH7 anion-exchange membranes and without membrane. More details can be found in Table S1.

processes of LiCl, NaCl and KCl were compared, as shown in Fig. 5.

It can be seen that the MCDI stack with 10THF7 membrane was able to adsorb more LiCl than the system with 9CH7 membrane. The kinetics of LiCl adsorption was the fastest for both systems and maximum uptake of LiCl reached 42.1 and 35.3 mg/g for stacks equipped with 10THF7 and 9CH7, respectively. Other salts were extracted slower and to the lower extent. Maximum salt adsorptions for stack with 10THF7 and 9CH7 membranes were 8.6 and 23.9 mg/g for KCl and 9.8 and 22.0 mg/g for NaCl, respectively.

The evaluation of electrode repeatability was conducted for MCDI system with 10THF7 and 9CH7 membranes. Fourteen cycle repetitions were carried out. The values of lithium chloride adsorption are shown in Fig. 6. It could be noted that the MCDI system kept adsorption capacity with low fluctuation of that value. The average values of salt adsorption were 34.14 and 26.86 mg/g LiCl for both evaluated membranes, respectively.

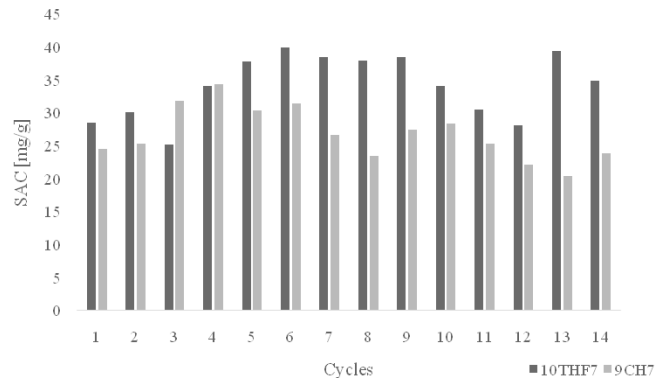


Fig. 6. Salt adsorption capacity of lithium chloride for cyclic process. Used voltage 2.5 V.

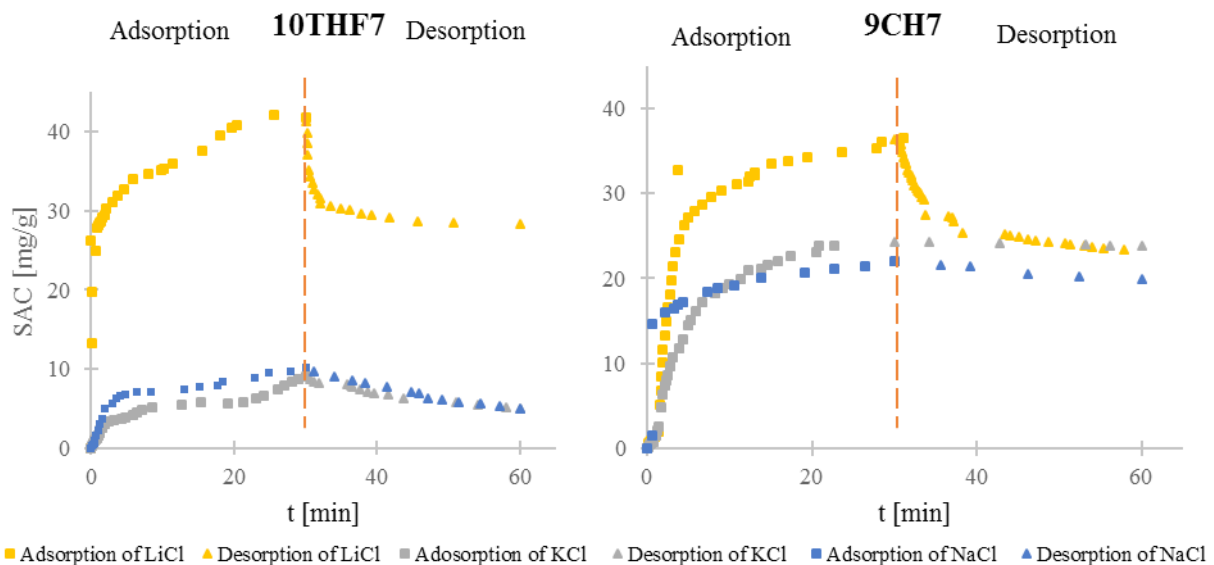


Fig. 5. Salt adsorption capacity in sorption and desorption processes for stacks with 10THF7 and 9CH7 membranes. Sorption at 2.5 V and desorption at 2.5 V. More details can be found in Table S2.

It can be summarized that the stack with 10THF7 membrane was more efficient for lithium ions extraction than stack with 9CH7 membrane. The observed phenomenon gave a chance to use the MCDI system to facilitate extraction of lithium chloride from multicomponent mixtures.

#### 4. Conclusion

The paper describes properties of new MCDI system used for lithium recovery from aqueous solutions. The stack consisted of non-coated electrode with lithium selective inorganic adsorbent and activated carbon electrode wrapped with PVC membrane modified with EDA. The best membrane for the separation process was prepared from solution of PVC in THF followed by the film modification with EDA. By using the MCDI system, it was possible to extract about 40 mg/g of lithium chloride when sodium chloride was extracted on the level of 10 mg/g.

#### Acknowledgment

The studies were supported by the Statutory Funds for Faculty of Chemistry, Wrocław University of Technology.

#### References

- [1] P. Meshram, B.D. Pandey, T.R. Mankhand, Extraction of lithium from primary and secondary sources by pre-treatment, leaching and separation: a comprehensive review, *Hydrometallurgy*, 150 (2014) 192–208.
- [2] R. Trocoli, G.K. Bidhendi, F. La Mantia, Lithium recovery by means of electrochemical ion pumping: a comparison between salt capturing and selective exchange, *J. Phys.: Condens. Matter*, 28 (2016) 114005.
- [3] L.T. Peiro, G.V. Mendez, R.U. Ayres, Lithium: sources, production, uses, and recovery outlook, *JOM*, 65 (2013) 986–996.
- [4] M. Bryjak, A. Siekierka, J. Kujawski, K. Smolinska-Kempisty, W. Kujawski, Capacitive deionization for selective extraction of lithium from aqueous solutions, *J. Membr. Sep. Technol.*, 4 (2015) 110–115.
- [5] H.J. Park, N. Singhal, E.H. Jho, Lithium sorption properties of HMnO in seawater and wastewater, *Water Res.*, 87 (2015) 320–327.
- [6] S. Nishihama, K. Onishi, K. Yoshizuka, Selective recovery process of lithium from seawater using integrated ion exchange methods, *Solvent Extr. Ion Exch.*, 29 (2011) 421–431.
- [7] J. Park, H. Sato, S. Nishihama, K. Yoshizuka, Lithium recovery from geothermal water by combined adsorption methods, *Solvent Extr. Ion Exch.*, 30 (2012) 398–404.
- [8] J. Lemaire, L. Svecova, F. Lagallarde, R. Laucournet, P.X. Thivel, Lithium recovery from aqueous solution by sorption/desorption, *Hydrometallurgy*, 143 (2014) 1–11.
- [9] J.L. Xiao, S.Y. Sun, X. Song, P. Li, J.G. Yu, Lithium ion recovery from brine using granulated polyacrylamide–MnO<sub>2</sub> ion-sieve, *Chem. Eng. J.*, 279 (2015) 659–666.
- [10] R. Chitrakar, H. Kanoh, Y. Miyai, K. Ooi, Recovery of lithium from seawater using manganese oxide adsorbent (H<sub>1.6</sub>Mn<sub>1.6</sub>O<sub>3</sub>) derived from Li<sub>1.6</sub>Mn<sub>1.6</sub>O<sub>4</sub>, *Ind. Eng. Chem. Res.*, 40 (2001) 2054–2058.
- [11] S. Cotte, B. Pecquenard, F. Le Cras, R. Grissa, H. Martinez, L. Bourgeois, Lithium-rich manganese oxide spinel thin films as 3 V electrode for lithium batteries, *Electrochim. Acta*, 180 (2015) 528–534.
- [12] S. Umetani, K. Maeda, S. Kihara, M. Matsui, Solvent extraction of lithium and sodium with 4-benzoyl or 4-perfluoroacyl-5-ryrazolone and TOPO, *Talanta*, 34 (1987) 779–782.
- [13] K. Ishimori, H. Imura, K. Ohashi, Effect of 1,10-phenanthroline on the extraction and separation of lithium(I), sodium(I) and potassium(I) with thenoyltrifluoroacetone, *Anal. Chim. Acta*, 454 (2002) 241–247.
- [14] C. Shi, D. Duan, Y. Jia, Y. Jing, A highly efficient solvent system containing ionic liquid in tributyl phosphate for lithium ion extraction, *J. Mol. Liq.*, 200 (2014) 191–195.
- [15] K. Onishi, T. Nakamura, S. Nishihama, K. Yoshizuka, Synergistic solvent impregnated resin for adsorptive separation of lithium ion, *Ind. Eng. Chem. Res.*, 49 (2010) 6554–6558.
- [16] X. Liu, X. Chen, L. He, Z. Zhao, Study on extraction of lithium from salt lake brine by membrane electrolysis, *Desalination*, 376 (2015) 35–40.
- [17] M. Reig, H. Farrokhzad, B. Van der Bruggen, O. Gibert, J.L. Cortina, Synthesis of a monovalent selective cation exchange membrane to concentrate reverse osmosis brines by electro dialysis, *Desalination*, 375 (2015) 1–9.
- [18] M. Pasta, A. Battistel, F. La Mantia, Batteries for lithium recovery from brines, *Energy Environ. Sci.*, 5 (2012) 9487–9491.
- [19] C.W. Hwang, M.H. Jeong, Y.J. Kim, W.K. Son, K.S. Kang, C.S. Lee, T.S. Hwang, Process design for lithium recovery using bipolar membrane electro dialysis system, *Sep. Purif. Technol.*, 166 (2016) 34–40.
- [20] S. Kim, J. Lee, J.S. Kang, K. Jo, S. Kim, Y.E. Sung, J. Yoon, Lithium recovery from brine using a  $\lambda$ -MnO<sub>2</sub>/activated carbon hybrid supercapacitor system, *Chemosphere*, 125 (2015) 50–56.
- [21] T. Ryu, G.H. Lee, J.C. Ryu, J. Shin, K.S. Chung, Y.H. Kim, Lithium recovery system using electrostatic field assistance, *Hydrometallurgy*, 151 (2015) 78–83.
- [22] E. García-Quismondo, C. Santos, J. Palma, M.A. Anderson, On the challenge of developing wastewater treatment processes: capacitive deionization, *Desal. Water Treat.*, 57 (2016) 2315–2324.
- [23] S. Porada, R. Zhao, A. van der Wal, V. Presser, P.M. Biesheuvel, Review on the science and technology of water desalination by capacitive deionization, *Prog. Mater. Sci.*, 58 (2013) 1388–1442.
- [24] X. Gao, S. Porada, A. Omosebi, K.L. Liu, P.M. Biesheuvel, J. Landon, Complementary surface charge for enhanced capacitive deionization, *Water Res.*, 92 (2016) 275–282.
- [25] P.M. Biesheuvel, H.V.M. Hamelers, M.E. Suss, Theory of water desalination by porous electrodes with immobile chemical charge, *Colloids Interface Sci. Commun.*, 9 (2015) 1–5.
- [26] X. Gao, A. Omosebi, J. Landon, K. Liu, Surface charge enhanced carbon electrodes for stable and efficient capacitive deionization using inverted adsorption–desorption behavior, *Energy Environ. Sci.*, 8 (2015) 897–909.
- [27] X. Gao, A. Omosebi, J. Landon, K. Liu, Enhanced salt removal in an inverted capacitive deionization cell using amine modified microporous carbon electrode, *Environ. Sci. Technol.*, 49 (2015) 10920–10926.
- [28] M.A. Anderson, A.L. Cudero, J. Palma, Capacitive deionization as an electrochemical means of saving energy and delivering clean water. Comparison to present desalination practices: will it compete?, *Electrochim. Acta*, 55 (2010) 3845–3856.
- [29] J.J. Wouters, J.J. Lado, M.I. Tejedor-Tejedor, R. Perez-Roa, M.A. Anderson, Carbon fiber sheets coated with thin-films of SiO<sub>2</sub> and  $\gamma$ -Al<sub>2</sub>O<sub>3</sub> as electrodes in capacitive deionization: relationship between properties of the oxide films and electrode performance, *Electrochim. Acta* 112 (2013) 763–773.
- [30] J. Liu, M. Lu, J. Yang, J. Cheng, W. Cai, Capacitive desalination of ZnO/activated carbon asymmetric capacitor and mechanism analysis, *Electrochim. Acta*, 151 (2015) 312–318.
- [31] J.J. Lado, R.E. Pérez-Roa, J.J. Wouters, M.I. Tejedor-Tejedor, M.A. Anderson, Evaluation of operational parameters for a capacitive deionization reactor employing asymmetric electrodes, *Sep. Purif. Technol.*, 133 (2014) 236–245.
- [32] J. Yang, L. Zou, N.R. Choudhury, Ion-selective carbon nanotube electrodes in capacitive deionisation, *Electrochim. Acta*, 91 (2013) 11–19.
- [33] T. Wu, G. Wang, F. Zhan, Q. Dong, Q. Ren, J. Wang, J. Qiu, Surface-treated carbon electrodes with modified potential of zero charge for capacitive deionization, *Water Res.*, 93 (2016) 30–37.
- [34] P.M. Biesheuvel, A. van der Wal, Membrane capacitive deionization, *J. Membr. Sci.*, 346 (2010) 256–262.
- [35] T. Ryu, J.C. Ryu, J. Shin, D.H. Lee, Y.H. Kim, K.S. Chung, Recovery of lithium by an electrostatic field-assisted desorption process, *Ind. Eng. Chem. Res.*, 52 (2013) 13738–13742.

- [36] J. Wolska, K. Wieluchowski, K. Helios, Ion-Exchange Membranes from Poly(Vinyl Chloride), R. Steller, D. Zuchowskiej, Eds., Proc. Conference Polymer Modification, TEMPO, Wrocław, 2015, pp. 471–474.
- [37] P. Cyganowski, D. Jermakowicz-Bartkowiak, J. Chęcmanowski, An assessment of a new synthetic procedure for core-shell polymeric supports based on the Amberlite XAD-4 adsorbent, *Acta Chim. Slov.*, 62 (2015) 672–678.
- [38] D. Jermakowicz-Bartkowiak, P. Cyganowski, Effect of microwave radiation on the synthesis of ion exchange resins: a comparative study, *Solvent Extr. Ion Exch.*, 33 (2015) 510–521.
- [39] E. Yavuz, Y. Gursel, B.F. Senkal, Modification of poly(glycidyl methacrylate) grafted onto crosslinked PVC with iminopropylene glycol group and use for removing boron from water, *Desalination*, 310 (2013) 145–150.
- [40] Z. Zhang, Effect of External Electric Field on Hydrogen Adsorption over Activated Carbon Separated by Dielectric Materials, PhD Thesis, Michigan Technological University, 2012.

## Supplementary data

Table S1

Salt adsorption capacity (SAC) of lithium chloride in CDI and MCDI stack with 10THF7 and 9CH7 anion-exchange membranes and without membrane

Voltage (V)	SAC (mg/g), 10THF7			SAC (mg/g), 9CH7			SAC (mg/g), without membrane			$\overline{\text{SAC}}$ (mg/g), 10THF7	$\overline{\text{SAC}}$ (mg/g), 9CH7	$\overline{\text{SAC}}$ (mg/g), without membrane
0.5	21.4	22.7	19.8	16.4	15.2	13.7	14.7	15.4	17.9	21.3	15.1	16.0
1	28.7	28.6	26.1	18.7	16.0	13.7	20.4	21.7	20.7	27.8	16.1	20.9
1.5	32.9	30.9	29.5	25.6	23.6	20.7	22	23.4	21.7	31.1	23.3	22.3
2	37.4	36.1	35.8	31.8	27.1	22.8	24.8	26.1	25.0	36.4	27.2	25.3
2.5	41.8	39.7	37.1	36.5	31.6	28.5	26.2	27.9	27.1	39.5	32.2	27.0
3	38.9	35.9	34.5	32.7	30.7	24.6	25.6	26.3	25.8	36.4	29.3	25.9

Table S2

Electrosorption capacity in sorption and desorption processes for stacks with 10THF7 and 9CH7 membranes

Time (s)	Temporary SAC (mg/g)	Time (s)	Temporary SAC (mg/g)	Time (s)	Temporary SAC (mg/g)
Measurement solution: LiCl		Measurement solution: KCl		Measurement solution: NaCl	
9CH7 adsorption					
0	0.000	0	0	0	0.000
8	0.649	4	0.216	34	1.486
18	0.811	13	0.432	40	14.595
29	0.973	28	0.649	132	15.946
41	1.135	43	0.757	193	16.486
58	1.297	50	1.189	225	16.892
84	1.946	60	1.514	260	17.162
90	5.189	72	2.054	438	18.378
97	6.811	80	2.595	515	18.784
102	8.432	98	4.757	638	19.189
108	10.054	111	6.378	826	20.000
114	11.676	126	7.459	1,143	20.676
131	13.297	135	8.000	1,360	21.081
142	14.919	145	8.541	1,586	21.486
151	16.541	168	9.622	1,800	22.027
163	18.162	190	10.703		
174	19.784	230	11.784		
188	21.405	260	12.865		
204	23.027	300	14.486		
231	24.649	320	15.027		
268	26.270	353	16.108		
301	27.081	403	17.189		
346	27.892	495	18.270		
398	28.703	546	18.811		
466	29.514	597	19.351		
540	30.324	680	19.892		

(Continued)



Table S2 (Continued)

Time (s)	Temporary SAC (mg/g)	Time (s)	Temporary SAC (mg/g)	Time (s)	Temporary SAC (mg/g)
Measurement solution: LiCl		Measurement solution: KCl		Measurement solution: NaCl	
650	31.135	738	20.973		
732	31.297	834	21.189		
746	31.946	873	21.514		
785	32.108	950	22.054		
787	32.432	1,047	22.595		
223	32.757	1,229	23.135		
907	33.405	1,246	23.784		
1,023	33.730	1,366	23.892		
1,168	34.216	1,800	24.216		
1,420	34.865				
1,670	35.351				
1,711	36.000				
1,867	36.486				
9CH7 desorption					
0	36.476	0	24.324	0	22.027
36	36.324	249	24.216	340	21.622
44	36.162	768	24.108	549	21.351
50	35.676	1,395	24.000	975	20.541
56	35.189	1,570	23.892	1,347	20.135
64	34.865	1,800	23.784	1,800	19.865
71	34.216				
77	33.892				
83	33.568				
93	33.405				
106	32.757				
118	32.432				
125	32.108				
131	31.784				
145	31.459				
158	30.973				
165	30.649				
181	30.324				
186	30.162				
193	30.000				
212	29.514				
222	29.189				
391	27.405				
423	27.243				
433	27.081				
493	26.757				
800	25.297				
843	25.135				
905	24.973				
976	24.811				
1,031	24.649				
1,125	24.486				
1,239	24.324				
1,282	24.162				

(Continued)

Table S2 (Continued)

Time (s)	Temporary SAC (mg/g)	Time (s)	Temporary SAC (mg/g)	Time (s)	Temporary SAC (mg/g)
Measurement solution: LiCl		Measurement solution: KCl		Measurement solution: NaCl	
1,380	24.000				
1,442	23.838				
1,520	23.676				
1,675	23.514				
1,772	23.351				
1,800	23.231				
10THF7 adsorption					
0	0.000	0	0.000	0	0.000
7	13.297	10	0.324	11	0.270
10	19.784	14	0.649	19	0.405
41	24.973	27	0.865	28	0.541
44	26.270	34	0.973	34	0.946
47	27.892	39	1.081	44	1.622
60	28.216	47	1.297	59	2.297
74	28.541	58	1.514	67	2.973
84	28.703	64	1.622	89	3.649
91	29.189	68	1.946	120	5.000
110	29.514	71	2.270	175	5.676
129	30.324	89	2.595	210	6.351
175	31.135	111	3.027	243	6.622
221	31.946	147	3.351	286	6.757
271	32.757	194	3.568	379	7.027
354	34.054	256	3.676	501	7.162
482	34.703	289	3.892	782	7.432
583	35.189	356	4.108	912	7.703
610	35.351	380	4.432	1,059	7.973
687	36.000	429	4.757	1,100	8.378
929	37.622	510	5.081	1,376	8.919
1,088	39.568	759	5.514	1,496	9.459
1,177	40.541	920	5.730	1,670	9.730
1,225	40.865	1,150	5.622	1,800	10.135
1,540	42.162	1,276	5.838		
1,800	41.838	1,380	6.270		
		1,450	6.595		
		1,564	7.351		
		1,623	7.892		
		1,689	8.432		
		1,740	8.649		
		1,800	9.081		
10THF7 desorption					
0	41.838	0	9.081	0	10.135
4	41.351	41	8.649	67	9.730
10	39.892	68	8.432	245	9.054
14	38.595	110	8.216	390	8.514
19	37.135	348	8.000	501	8.243
26	35.189	380	7.892	678	7.703
35	34.378	390	7.784	890	7.162
53	33.568	460	7.351	950	6.892

(Continued)

Table S2 (Continued)

Time (s)	Temporary SAC (mg/g)	Time (s)	Temporary SAC (mg/g)	Time (s)	Temporary SAC (mg/g)
Measurement solution: LiCl		Measurement solution: KCl		Measurement solution: NaCl	
72	32.757	520	7.135	1,023	6.351
98	32.108	578	6.919	1,146	6.081
118	31.622	689	6.703	1,287	5.811
122	30.973	826	6.270	1,470	5.676
204	30.649	1,259	5.730	1,631	5.270
299	30.324	1,450	5.405	1,800	5.000
372	30.162	1,680	5.189		
465	29.676	1,800	4.973		
550	29.514				
705	29.189				
939	28.703				
1,237	28.541				
1,800	28.378				

Note: LiCl, KCl or NaCl in feeding phase. Sorption at 2.5 V and desorption at 0.5 V.